Available online at www.sciencedirect.com
ScienceDirect
International Journal of Pharmaceutics 332 (2007) 168–175
INTERNATIONAL JOURNAL OF PHARMACEUTICS
www.elsevier.com/locate/ijpharm

Pharmaceutical Nanotechnology

Elastic modulus measurements from individual lactose particles using atomic force microscopy

Mark Perkins [a], Stephen J. Ebbens [a], Simon Hayes [b], Clive J. Roberts [a], Claire E. Madden [a], Shen Y. Luk [a], Nikin Patel [a,*]

[a] *Molecular Profiles Ltd., 8 Orchard Place, Nottingham Business Park, Nottingham NG8 6PX, UK*
[b] *University of Sheffield, Department of Engineering Materials, Sheffield, Yorkshire S1 3JD, UK*

Received 12 June 2006; received in revised form 19 September 2006; accepted 21 September 2006
Available online 26 September 2006

Abstract

The elastic modulus of pharmaceutical materials affects a number of pharmaceutical processes and subsequently formulation performance and is currently assessed by bulk methods, such as beam bending of compacts. Here we demonstrate the accurate measurement of the elastic modulus of alpha monohydrate lactose from the dominant (0 1 1) face of single crystals using atomic force microscopy (AFM) as 3.45 ± 0.90 GPa. The criteria to ensure this data is recorded within the elastic limit and can be modelled using Hertzian theory are established. We compare and contrast this AFM method to a permanent indentation technique based upon a much larger Berkovich pyramidal indenter on a lactose compact and the wider literature. Finally the AFM was utilized to study the elastic response of amorphous lactose, demonstrating that the physical state of the amorphous material changes under repeated loading and behaves in a more crystalline manner under repeated force measurements, suggesting a pressure induced phase transition. The AFM based approach demonstrated has the significant advantages of requiring minimal sample, no need for producing a compact, being non-destructive in that no permanent indent is required and providing a technique capable of detecting variations in material properties across a single particle or a number of particles.

Keywords: Atomic force microscopy; Elastic modulus; Lactose; Nanoindentation

1. Introduction

The deformation behaviour of pharmaceutical ingredients is known to affect pharmaceutical processes such as milling and compaction (Liao and Wiedmann, 2005; Kwan et al., 2004; Jain, 1999; Narayan and Hancock, 2003) and hence subsequently formulation performance. As a consequence, there is interest in methods that can be used to extract quantitative measures of these properties. Youngs' modulus and other commonly quoted parameters have been determined from bulk methods such as beam-bending (Podczeck, 2001), however there are disadvantages with this macroscopic approach. Even using miniaturised beams, milligram quantities of material are required, preventing screening of active pharmaceutical ingredients at early stages of development (Hancock et al., 2000). In addition, the methodology of beam-bending relies on assumptions including extrapolation to zero porosity. This has been shown to result in large magnitude differences in reported data (BinBaie et al., 1996).

To overcome these issues, techniques using atomic force microscopy (AFM) capable of performing measurements on individual active pharmaceutical ingredients (API) and excipient particles have been developed (Roberts, 2005). These methods have until now been broadly termed "nanoindentation". To date, most reported pharmaceutical examples of this approach have used a modified atomic force microscope equipped with a relatively large probe with well defined geometry and a much stiffened spring that supports this probe (Liao and Wiedmann, 2005; Taylor et al., 2004; Liao and Wiedmann, 2004). Typically in these methods material parameters are extracted from load–displacement unloading curves using approaches outlined by Oliver and Pharr (1992). One example showed the ability to measure the modulus and fracture toughness of five different pharmaceutical materials (Taylor et al., 2004). Another study measured changes in material properties occurring during the

* Corresponding author. Tel.: +44 115 871 8888; fax: +44 115 871 8889.
E-mail address: npatel@molprofiles.co.uk (N. Patel).

0378-5173/$ – see front matter © 2006 Elsevier B.V. All rights reserved.
doi:10.1016/j.ijpharm.2006.09.032

recrystallisation of acetaminophen and related these to structural differences revealed using AFM imaging (Liao and Wiedmann, 2005). The use of the term "nanoindentation" to describe these methods is questionable, as analysis often results in permanent indentations that are 10–15 μm in size, and can cause crystals to fracture (Taylor et al., 2004). The potential for damage to the sample, combined with the large probe size, significantly reduces the ability to map elastic modulus variations across crystal faces, and significantly lowers topographical image quality.

To overcome the drawbacks of poor image quality and damage to the sample, an alternative strategy is needed. Image resolution can be improved by using the sharper probes employed for conventional AFM imaging experiments. Furthermore, if conditions are chosen carefully it is possible to probe surface material properties such as elastic modulus using the probe to cause small reversible deformations, not exceeding the elastic limit of the sample. In this situation, Hertzian mechanics can be applied, allowing the elastic modulus to be obtained from the loading curves. To date, this approach has been successful for a range of soft to medium stiffness materials including cells and polymers (Bowen et al., 2000; Du et al., 2001). In addition, we have recently shown the capability of this method to distinguish amorphous and crystalline domains at the surface of a compact of sorbitol (Ward et al., 2005). This true nanoindentation method has the capability to be non-destructive and map variations in mechanical properties on the nanoscale (Heuberger et al., 1995). In addition this method does not require modification of conventional AFM platforms, and can be combined with high resolution topographical imaging in tapping and contact mode.

In this work, we investigate the applicability of this later approach to measuring the elastic modulus of crystalline and amorphous lactose with an emphasis on making measurements on single particles. Particular thought is given to assessing if these materials can be probed in a way that generates data conforming to the Hertz criteria. In addition a more established method of nanoindentation will be compared, that operates at much higher forces and probe sizes.

2. Materials and methods

Alpha lactose monohydrate (Respitose SV001 from DMV, Veghel, Netherlands) was recrystallised according to the solvent evaporation method described by Begat et al. (2004) to produce smooth crystals suitable for elastic modulus testing. Samples were analysed as prepared. It was found that the crystals made intimate contact with a glass support, and so were rigidly supported during force distance measurements. To produce amorphous lactose, the crystalline material was spray-dried from a 10% (w/v) solution using a Buchi minispray drier 190 with an inlet temperature of 166 °C, an outlet temperature of 97 °C, and a flow rate of 13 mL min^{-1} to generate an amorphous sample (Zhang et al., 2006). The spray-dried lactose was proved to be amorphous using powder X-ray diffraction (PXRD) with a Philips, X-pert Diffractometer instrument. This material was stored under a phosphorous pentoxide desiccant prior to analysis. To facilitate AFM data acquisition from the spray-dried amorphous lactose, the sample was prepared in a disk form by pressing the sample powders into a die (Specadie, Specac Ltd., Kent, UK). The infrared spectra of the spray dried powder (characterised as amorphous by PXRD) and the pressed disk were identical (Smart Golden Gate, Avatar 370 FT-IR, Thermo Nicolet, Madison, WI, USA). This shows that the surface of the pressed disk to a depth of (approximately 1 μm) is still in an amorphous state. The bands used for comparison were those in the O–H stretch region which is sensitive to both the alpha- and beta-crystalline phases (peaks at 3522 cm^{-1} for the alpha phase, and 3437 cm^{-1} for the beta phase) (Drapier-Beche and Parmentier, 1999). In order to increase the sensitivity for infrared spectroscopy, the second derivative spectra were examined and this shows that the spectra are free from lactose in alpha and beta crystalline phase.

Scanning electron microscopy (SEM) was carried out using a Leo 1430VP Electron microscope. The accelerating voltage was 10 kV, at a working distance of 10 mm.

AFM images were acquired on a Multimode AFM (Veeco, Santa Barbara, CA) using TESP Silicon cantilevers (Veeco, nominal spring constant = 42 N m^{-1}) operating in tapping mode. The spring constant were calculated using the Sader method (1995). Resonance frequencies were approximately 270 kHz, the set-point ratio used was 0.7 (Bar et al., 2000) and scan rates were typically 1–2 Hz. Some probes were pre-blunted by scanning against a hard substrate such as silicon or glass. AFM force–distance curves, used to derive nanomechanical properties, were collected on the same instrument. Data was acquired from at least four crystals (20 force distance measurements) using the blunted probes and at least three crystals (25 force distance measurements) using the sharp probes. Where multiple measurements were made on a single crystal the probe was repositioned each time.

In addition to the curves recorded on the lactose crystals and the amorphous material, force–distance curves were obtained from the glass support to provide an ideally hard reference material. Each data set was recorded using the same instrumental adjustments and experimental parameters.

In a typical experiment, a suitable area was located using an optical microscope attached to the AFM set-up and the region was imaged using tapping mode. In the case of the crystalline material these regions were selected from the dominant (0 1 1) face of the crystal. The instrument was then switched to contact mode and re-engaged in the same location to record force-distance curves. Each individual force-distance curve was laterally separated by at least 1 μm from the preceding measurement to ensure that the observations are independent. Finally, the AFM was re-engaged in tapping mode, and the area of analysis was re-imaged to assess if the measurements had been performed non-destructively.

A comparison of the gradients of the contact region of the force–distance curves between a hard non-deformable reference surface and the sample can provide some qualitative indication of the relative stiffness of a surface (Radmacher et al., 1994). This can be modelled using the Hertz model to obtain a quantitative value of the elastic modulus of the surface. The model describes the elastic deformation of two homogenous surfaces

under an applied load and is often used to model AFM data since it requires little knowledge of parameters such as surface energy. The first step in modelling the data is to compare force–distance curves recorded on the sample and the ideally hard reference (glass surface) to determine the indentation (δ) of the probe into the lactose sample as a function of load. The contact regions of the curves are overlaid such that zero force is equal to zero indentation.

The value of indentation can be related to the combined elastic modulus of the tip and the sample (K) by:

$$K = \frac{L}{(8\delta^3 R)^{1/2}} \tag{1}$$

where L is the load and R is the radius of the probe. Since the combined elastic modulus contains the elastic moduli for the tip and the sample, an expression containing the E_s, the elastic moduli of the sample can be obtained:

$$K = \frac{4}{3}\left(\frac{1-\nu_t^2}{E_t} + \frac{1-\nu_s^2}{E_s}\right)^{-1} \tag{2}$$

where ν_t and ν_s are the Possions' ratio of the tip and the sample, respectively. Since E_t is much greater than E_s the first bracketed term of Eq. (2) may be ignored to produce Eq. (3):

$$E_s = \frac{3K(1-\nu_s^2)}{4} \tag{3}$$

Combining Eqs. (1) and (3) derives:

$$E_s = \frac{3L(1-\nu_s^2)}{4(8\delta^3 R)^{1/2}} \tag{4}$$

The value of ν_s is difficult to determine accurately for many samples including single crystals such as those investigated here. Therefore it is appropriate to use a midrange value of ν_s (typical range is from 0.1 to 0.5) since varying this has little effect of the value obtained for E_s. Here we have assumed a value of ν_s to be 0.3. R is deduced from the tip profile determined using a morphological tip derivation algorithm (Williams et al., 1996, 1998). R was checked before and after each measurement.

The Hertz model is valid only for elastic deformation so it is important to remove any contribution from inelastic deformation from the analysis. The model also assumes no significant adhesion between the probe and sample. To overcome this only data from the loading curve was used. To assess the validity of the data for use with the Hertz model, a plot of load versus indentation was produced. In the ideal situation a linear relationship between load and indentation will be observed to allow E_s to be calculated from the entire data set. In some instances this linear relationship was only seen for a small range of forces. These regions can be selected as the elastic region and partial fit of the data can be carried out between a minimum and maximum load.

Conventional nanoindentation testing was performed using a Hystitron Triboscope (Scanwel, UK) interfaced with a DI Dimension 3100 AFM (Veeco). In this arrangement, a Hysitron supplied scanner and transducer replaces the scanner and tip of the AFM. This arrangement was designed to provide highly reproducible indentation measurements, while maintaining a degree of imaging capability as a low resolution contact-mode AFM.

In this study, a Berkovich pyramidal indenter was used, which had a radius of approximately 100 nm at the tip. However, the Berkovich tip is a relatively flat three sided pyramidal tip, which can be approximated to a cone with an included angle of 140.6°. Therefore, this tip shape is prone to tip-induced artefacts when imaging surfaces that are less than ideally smooth, as the sides of the tip can easily contact asperities and make them appear larger than they are, and pyramidal in shape. However, the Berkovich tip is commonly used as the standard tip geometry in nanoindentation, as it has the same conic-section as the Vickers indenter as used in conventional materials testing, and therefore allows data to be readily compared between nano-, micro- and macro-modulus tests.

When analysing the lactose compact, a repeated load/unload cycle was applied, with progressively larger indent loads applied on each cycle. This was used to examine whether the depth of an indent affected the measured modulus of the compacted sample. The data was analysed using the conventional Oliver and Pharr approach, as contained in the Hysitron software. This approach is based around the work of Sneddon (1965) who described that for many punch geometries the load displacement behaviour can be described by Eq. (5).

$$P = \alpha h^m \tag{5}$$

where P is the indenter load, h the elastic displacement and α and m are the constants. Where some plasticity is observed modelling this behaviour becomes more complex. Oliver–Pharr described the power law relationship (Eq. (6)).

$$P = A(h - h_f)^m \tag{6}$$

where P is the load, $(h - h_f)$ the elastic displacement, A and m are the material constants. This analysis assumes that only elastic deformation occurs in the initial stages of the unload curve, and therefore determines the sample modulus from this region. However, in the event of non-ideal deformations occurring, this assumption may not be true. The repeated load/unload cycle is valid in the Oliver and Pharr analysis, as only the initial elastic portion of the curve is analysed, but only in the event that no morphological changes occur in the sample.

3. Results and discussion

A scanning electron micrograph and a higher resolution AFM image of a re-crystallised lactose crystal are shown in Fig. 1. The crystal presents a smooth trapezoid shape, suitable for analysis. The crystal is composed of underlying columnar structures, which occasionally also produce topography at the exposed surface. It was possible to avoid these regions optically to ensure analysis was performed on an intact, continuous smooth surface. These large faces correspond to the dominant (0 1 1) plane of the crystal.

Elastic modulus measurements were undertaken with probes using a range of radius values. AFM probe radii were determined using tip-reconstruction algorithms (Williams et al., 1998). An

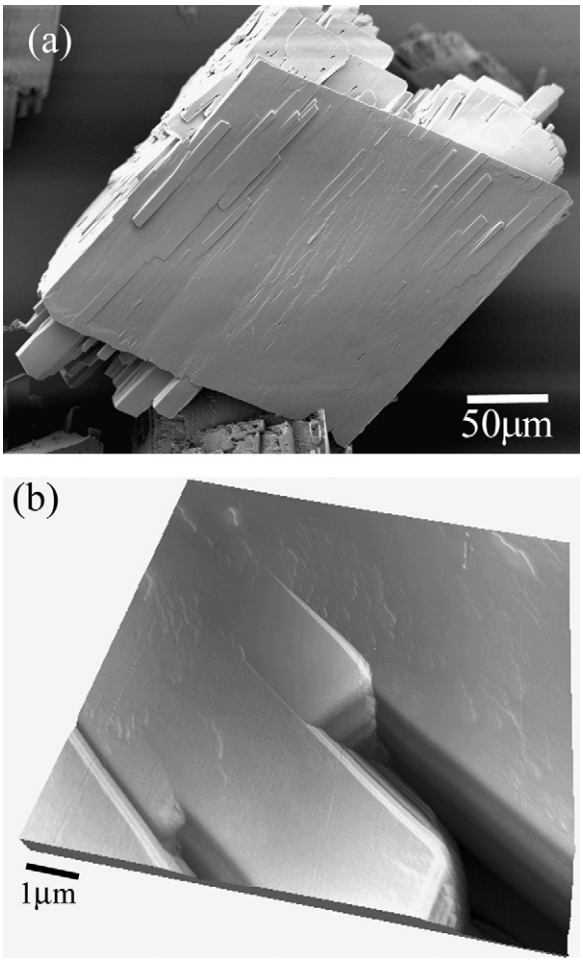

Fig. 1. (a) An SEM of a typical alpha monohydrate lactose crystal selected for elastic modulus analysis. (b) A 10 μm × 10 μm AFM image from the dominant (0 1 1) face of an alpha monohydrate lactose crystal (*z*-scale 500 nm).

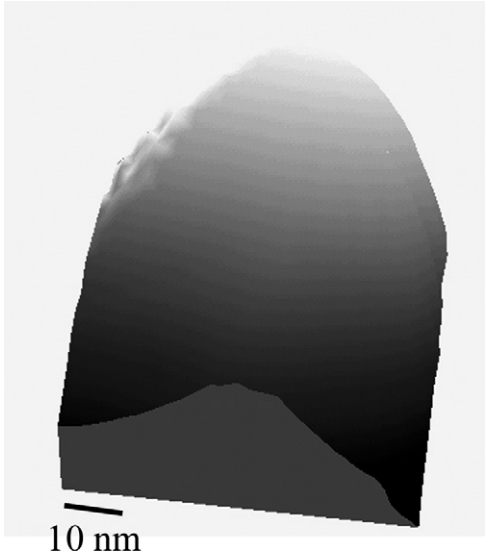

Fig. 2. An example of a reconstructed tip profile used for modulus testing. Here the tip has a terminal radius of 30 nm (*z*-scale 20 nm).

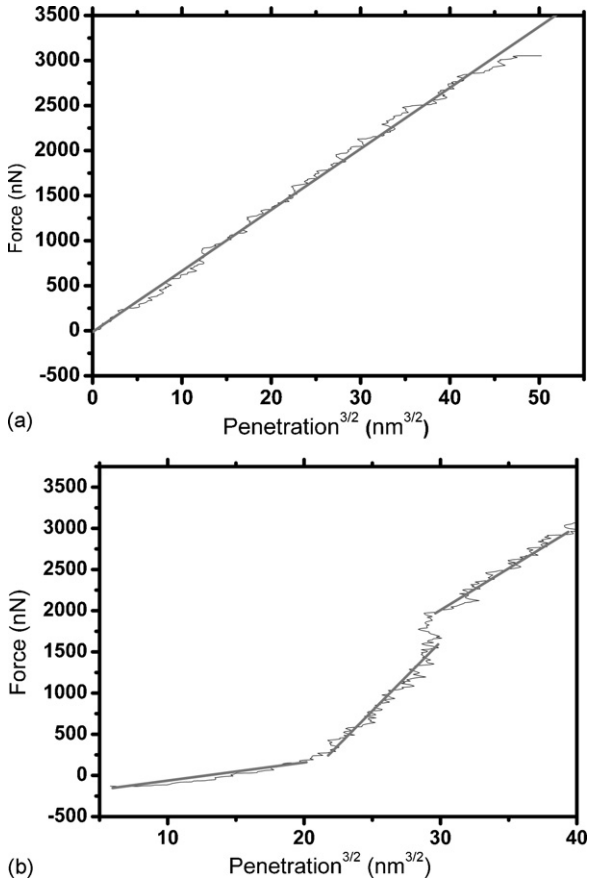

Fig. 3. (a) Force–penetration loading curve recorded from lactose (tip radius = 80 nm). (b) Force–penetration, loading curve exhibiting complex indentation/force behaviour (tip radius = 30 nm).

example of such a reconstructed tip-profile is shown in Fig. 2. Here we show data related to the use of tips with radii of 80 nm as an example of a relatively blunt probe, and 30 nm as an example of a sharper probe. Probes were evaluated both before and after indentation experiments. Significant changes in probe diameter were only detected in the sharp probes after continual use of 10 measurements or more. Fig. 3a and b illustrate typical derived force–penetration curves recorded with a probe of radius 80 nm and a probe of radius 30 nm, respectively. The linear regions of these plots indicate that the Hertzian model for a spherical probe contacting a planar substrate can be applied at these points. In the case of the 80 nm radius probe the force–indentation curve is linear over the entire loading range, indicating that the Hertzian conditions of reversible elastic deformation are achieved. This can be confirmed by subsequent tapping mode images of the region analysed, where no permanent indentations were apparent (data not shown). However, the load–indentation relationship observed for the sharper tip is much more complex, with a succession of linear regions observed, each with differing gradients, Fig. 3b. This data suggests that a more complex probe–sample interaction was occurring. This was confirmed by the observation that permanent indentations remain in the crystalline lactose sample after analysis with the sharper probe, as indicated by the pile up of material around the larger indent that can be seen in Fig. 4. It is of interest to note that the much smaller indent

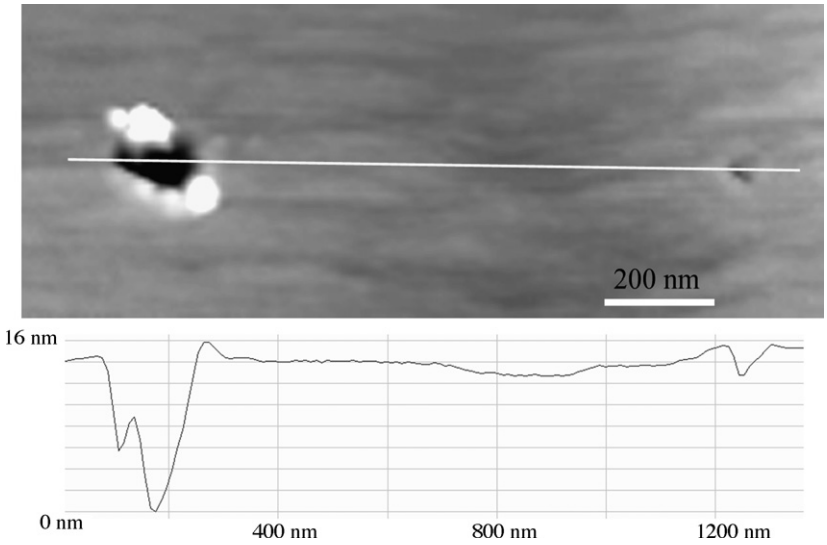

Fig. 4. Two indentations present after modulus testing with a tip radius = 30 nm (indentation depths are ~14 and 2 nm).

in this image was formed by an elastic modulus measurement with a reduced maximum loading (approximately 2.8 μN compared to 3.3 μN for the larger indent). Although the depth of the permanent indentations are small (ca. 15 nm for the larger and ca. 2 nm for the smaller) the forces applied by the probe have clearly resulted in permanent non-elastic deformations.

Whether Hertz conditions can be met in general in an AFM nanoindentation experiment will depend on the material under consideration and the stress applied by the probe. This later criteria is determined by two variables, the stiffness of the cantilever used and the probe geometry.

Ideal probe geometries for Hertz nanoindentation are well defined hemi-spheres of a reasonably large radius to reduce the possibility of exceeding the elastic limit of the material under analysis. This is seen here when using the blunted (80 nm) probe where we observed a much simpler relationship between the load and displacement curves. However, this consideration is balanced against the fact that large probes distribute the maximum load over a larger area. The results obtained under the same loading conditions with a sharper 30 nm radius probe, more typical of that used in AFM experiments, are more complex. The higher stresses applied by such probes caused the elastic limit to be exceeded and permanent indents to be formed, most likely at 1.5–2 μN loads where the largest non-linear region is seen in Fig. 3b and just above which the very small 2 nm deep indent shown in Fig. 4 was formed. It is likely that the exact form of the curves contain detailed information about the high stress behaviour of the sample, and may relate to the motion of underlying crystal planes in the structure. It should also be noted that these sharper probes demonstrated a significant change in probe radii after numerous measurements. The variance in mechanical response obtained between these probes and changes to the probe diameter illustrates the current difficulty in non-destructively testing pharmaceutical solids at high resolution.

It should be noted though that for the experiment to be optimal sufficient stress is needed to cause a deformation, and this may not be possible for large probe radius probes using standard (relatively low stiffness) AFM cantilevers. Consequently, at a given spring constant, larger radius probes set a potentially problematic lower limit on the maximum elastic modulus that can be measured.

Cantilever stiffness will determine the maximum amount of total force that can be applied to the sample and the force resolution of the data. At present, manufacturers cluster the stiffness of their probes around a range of values appropriate for imaging modes, so there is not a free choice of this parameter. Choosing an appropriately stiff cantilever is also hampered by the large amount of spread in spring constants of a given type, typically manufacturing tolerances are low, and spring constants can have up to a 100% uncertainty. This was observed here where the spring constants measured were typically 10–50% greater than the manufacturers value. The selection of suitable spring constants will in the future be aided by ongoing developments in force calibration samples and levers manufactured to tighter tolerances (Cumpson et al., 2004a,b). However, it does appear that with careful screening of probe spring constant and radius, reliable data can be obtained.

Table 1
Summary of elastic modulus results

Method	Model	Probe radius (nm)	Average modulus (GPa)	Standard deviation (GPa)
AFM	Hertz	79.8	3.45 ($n = 4$)	0.90
AFM	Hertz	34.6	5.4 ($n = 3$)	4.0
Hysitron	Power law	100	3–7 ($n = 3$)	–

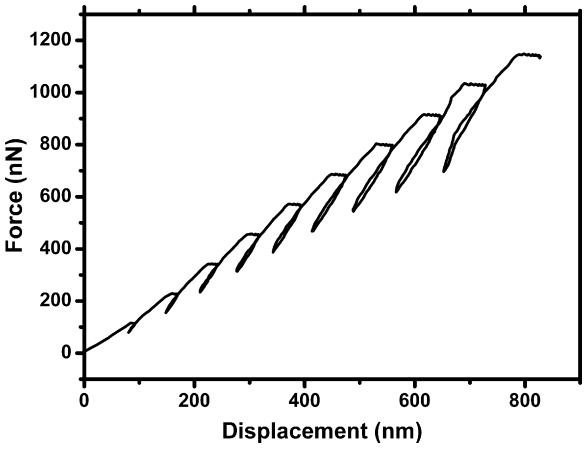

Fig. 5. Load–displacement curves recorded from a compressed alpha lactose monohydrate disc using a Hysitron indenter.

Having assessed the nature of the deformation caused by the probe it was possible to apply the Hertz model to determine the elastic modulus. Table 1 shows the average elastic modulus extracted from a number of force–distance curves recorded using both the sharp and blunter tip from a number of lactose crystals. Data recorded using the larger radius tip was modelled to give an elastic modulus of 3.45 ± 0.90 GPa. However, when applying the Hertzian model to data recorded with the sharper tip it was necessary to make a judgment about which linear region of the data to analyse. As it seems likely that load–displacement data recorded at lower forces will display Hertzian behaviour, the first significant linear section of each curve recorded using the sharp tip was selected and fitted to the Hertz model. This resulted in a higher mean elastic modulus of 5.4 ± 4.0 GPa, and an increased spread in the data compared to that recorded with the blunted probe.

To allow a comparison of this AFM based data with a more standard approach, a conventional "nanoindentation" experiment was also carried out on a pressed disc of the same crystalline lactose. Here, a succession of load–unload cycles with increasing maximum force were performed at a fixed location, Fig. 5. Due to the large probe size (~100 nm) and high included angle of the Berkovich tip, the resolution of accompanying AFM images recorded before and after the indentation cycles is much inferior to those achieved using the sharper probes, Fig. 6. In fact, it is likely that the tip shape greatly contributes to the structures observed in the images. However, it was possible to ascertain that there had been a gross permanent change in the surface structure of the lactose after testing, extending for several microns across the surface. Each unloading cycle was fitted to a power law, to enable elastic modulus values to be extracted. It was observed that the elastic modulus values reduced after each successive indentation with values ranging from 7.0 to 1.1 GPa extracted from the data. The conditions that are most similar to those used in the AFM experiment are present on the first load–unload cycle, with the lowest maximum force and a fresh surface. This curve gives a modulus value of 7 GPa in comparison with the values obtained from the AFM force-curves. Although the low amount of data considered in the Oliver and Pharr analysis for the unload portion of this curve makes the reliability of this value questionable. It may be the case that the subsequent values obtained in the second and third indents are the most representative, due to the greater amount of data available for curve fitting. Later data sets show distinct hysteresis, which is likely to be due to fracture of the pellet and frictional effects during loading. These later data points are therefore not ideal for analysis, as morphological changes in the sample are occurring. It is safest to say, therefore, that the modulus from conventional nanoindentation lies in the range of 3–7 GPa.

Table 2
Summary of reported lactose monohydrate modulus values

Method	Sample	Modulus (GPa)	Reference
Microindentation	Single crystal	1.52	Wong and Aulton (1993)
Beam bending	Compact	24.1	Bassam et al. (1991)
		7.7	Busignies et al. (2004)
		6.5	BinBaie et al. (1996)
		2.99	Podczeck (2001)

Previous methods to measure the elastic modulus of crystalline alpha lactose monohydrate have recorded values ranging

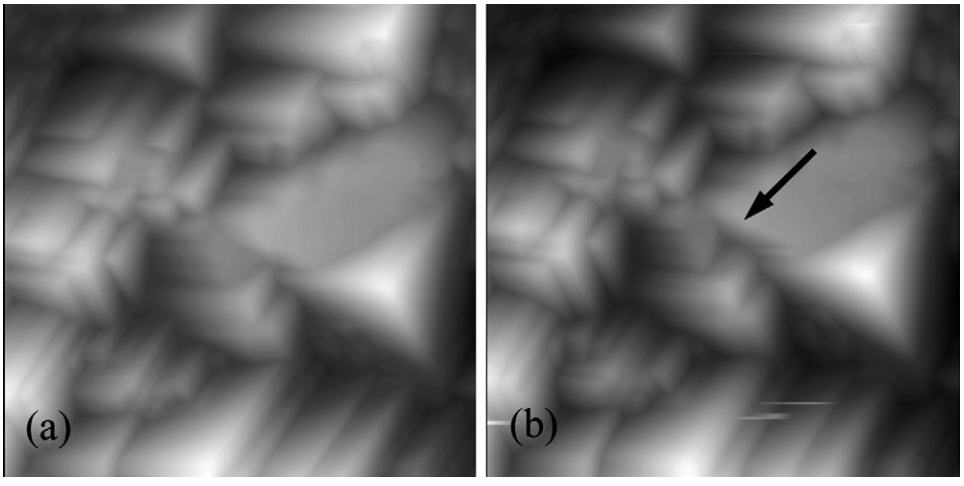

Fig. 6. Surface profile images recorded using the Hysitron indenter probe (a) before indentation; (b) after indentation, location of indent is marked with an arrow.

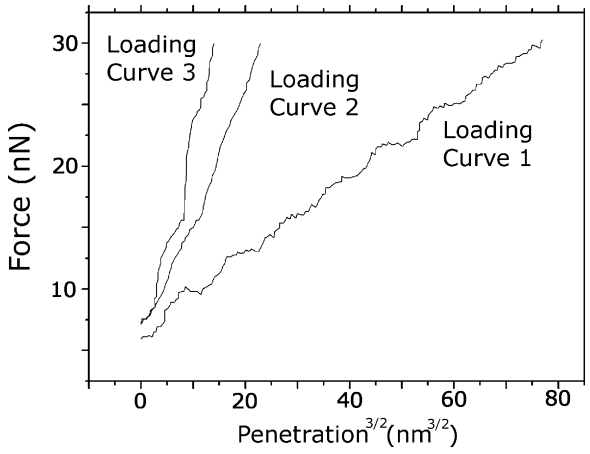

Fig. 7. Repeated force–penetration curves recorded at the same point on an amorphous lactose sample with a tip radius = 80 nm.

from 1.16 to 24.1 GPa (detailed in Table 2) compared to a value of 3.45 GPa as determined here. The spread in beam bending data has been partly attributed to particle size differences between samples, however it also illustrates the intrinsic difficulties in performing these experiments. The only reported value that considers an individual crystal was obtained using microindentation (1.16 GPa). This is the most directly comparable approach to that presented here, although this study used a much larger probe, with a radius of 340 μm, compared to the 80 nm probe used here and did not access a single crystal face.

The two more tightly grouped beam bending results (6.5 and 7.7 GPa) in Table 2 agree well with the presented Hysitron experiments on a solid compacted powder. The observation that applying successive loading cycles with increasing maximum force decreases the measured modulus suggests that significant changes are occurring to the compact during the measurement process. This was confirmed by the accompanying AFM data recorded at higher loadings, and also by the hysteresis apparent in the successive load/unload cycles of the Hysitron data.

Finally, the AFM method described was applied to a purely amorphous lactose sample. Using the 80 nm probe and a much reduced maximum loading of approximately 30 nN, repeated measurements were made at same position on the sample surface. An example of such data is shown in Fig. 7. Under these conditions the mechanical response of the amorphous lactose was clearly seen to change. Whilst a linear fit is still possible for each loading curve under these very low loading conditions, the elastic modulus of the sample increases with each measurement, being approximately 28 MPa on the first load curve, 86 MPa on the second and 210 MPa on the final measurement. This type of behaviour was consistent from all areas tested ($n = 4$).

The AFM nanoindentation data recorded from repeated measurements on a particular point of an amorphous lactose sample clearly indicates that the mechanical properties of the material are changing, showing an increase in elastic modulus with each measurement. In the wider literature plastic strain-induced phase changes under high pressure and plastic shear have been reported in a number of areas including geophysics and semiconductors (Levitas, 2004; Durandurdu and Drabold, 2003). This phenomena is less well studied in pharmaceuticals, although it is well known for example that the stresses of micronization can induce polymorphic conversion or amorphicity in a material (Brittain, 2002). Here it appears that stresses induced by the AFM probe, which equate to a maximum applied pressure in the region of 25 MPa, have been sufficient to alter the thermodynamically metastable amorphous state. It is tempting to suggest that the lactose is behaving in a more crystalline manner under repeated loading, since although the final elastic modulus remains roughly a factor of 10 less than that observed for the crystalline material it is clearly approaching a crystalline type mechanical response. Some justification for this proposal can be obtained if we consider that it is known that the required energy to transform bulk amorphous lactose to the crystalline state without nucleation and under non-isothermal conditions is 71 kJ mol^{-1} (Schmitt et al., 1999). The energy put into the surface by the AFM tip during an individual measurement was around 0.1 pJ and this was deposited in a volume of approximately 4×10^{-22} m^3, an energy density that equates to around 60 kJ mol^{-1}. This approximation is clearly subject to a number of assumptions but nevertheless the closeness of these values does at least suggest that the nanoscale transformation of amorphous lactose to a more crystalline state has taken place under the action of the AFM probe.

4. Conclusions

Here we have shown that using an unmodified AFM instrument with slightly blunted probes provides a reliable measure of elastic modulus for lactose in good agreement with the previous findings. More importantly the approach described here has the significant advantages of requiring no permanent indent and achieving a much improved spatial resolution, now limited by the curvature of a sharp probe (80 nm) rather than the large micron sized indentation probes currently used. This improved spatial resolution allows modulus measurements to be recorded from single particles and from specific crystal faces and hence opens the potential for the spatial mapping of elastic modulus, for example from different crystal faces or to identify local heterogeneities (e.g. amorphous domains). In this latter area any surface heterogeneity identified using AFM topographic (Davies et al., 1996) or phase imaging (Chen et al., 1998; Danesh et al., 2000) can now be investigated for corresponding elastic modulus variations. The elastic response of amorphous lactose was also characterized, with the material showing an indication of a pressure induced local recrystallization under the AFM probe.

Acknowledgments

Molecular Profiles would like to thank Prof. X. Chen and the Laboratory of Biophysics and Surface Analysis, School of Pharmacy, The University of Nottingham for valuable discussions and programming of the elastic modulus algorithms. In addition, we thank S. Evans and J. Zhang of Molecular Profiles for assistance with sample preparation and SEM analysis.

References

Bar, G., Ganter, M., Brandsch, R., Delineau, L., Whangbo, M.H., 2000. Examination of butadiene/styrene-co-butadiene rubber blends by tapping mode atomic force microscopy. Importance of the indentation depth and reduced tip-sample energy dissipation in tapping mode atomic force microscopy study of elastomers. Langmuir 16, 5702–5711.

Bassam, F., York, P., Rowe, R.C., Roberts, R.J., 1991. The young modulus of binary powder mixtures. Powder Technol. 65, 103–111.

Begat, P., Morton, D.A.V., Staniforth, J.N., Price, R., 2004. The cohesive-adhesive balances in dry powder inhaler formulations. I. Direct quantification by atomic force microscopy. Pharm. Res. 21, 1591–1597.

BinBaie, S., Newton, J.M., Podczeck, F., 1996. The characterization of the mechanical properties of pharmaceutical materials. Eur. J. Pharm. Biopharm. 42, 138–141.

Bowen, W.R., Lovitt, R.W., Wright, C.J., 2000. Application of atomic force microscopy to the study of micromechanical properties of biological materials. Biotechnol. Lett. 22, 893–903.

Brittain, H.G., 2002. Effects of mechanical processing on phase composition. J. Pharm. Sci. 91, 1573–1580.

Busignies, V., Tchoreloff, P., Leclerc, B., Besnard, M., Couarraze, G., 2004. Compaction of crystallographic forms of pharmaceutical granular lactoses. I. Compressibility. Eur. J. Pharm. Biopharm. 58, 569–576.

Chen, X., McGurk, S.L., Davies, M.C., Roberts, C.J., Shakesheff, K.M., Tendler, S.J.B., Williams, P.M., Davies, J., Dawkes, A.C., 1998. Chemical and morphological analysis of surface enrichment in a biodegradable polymer blend by phase-detection imaging atomic force microscopy. Macromolecules 31, 2278–2283.

Cumpson, P.J., Hedley, J., Clifford, C.A., Chen, X.Y., Allen, S., 2004a. Micro-electromechanical system device for calibration of atomic force microscope cantilever spring constants, between 0.01 and 4 N/m. J. Vac. Sci. Technol. A. 22, 1444–1449.

Cumpson, P.J., Clifford, C.A., Hedley, J., 2004b. Quantitative analytical atomic force microscopy: a cantilever reference device for easy and accurate AFM spring-constant calibration. Meas. Sci. Technol. 15, 1337–1346.

Danesh, A., Chen, X., Davies, M.C., Roberts, C.J., Sanders, G.W.H., Tendler, S.J.B., Williams, P.M., Wilkins, M.J., 2000. Polymorphic discrimination using atomic force microscopy: distinguishing between two polymorphs of the drug cimetidine. Langmuir 16, 866–870.

Davies, M.C., Shakesheff, K.M., Shard, A.G., Domb, A., Roberts, C.J., Tendler, S.J.B., Williams, P.M., 1996. Surface analysis of biodegradable polymer blends of poly(sebacic anhydride) and poly(DL-lactic acid). Macromolecules 29, 2205–2212.

Drapier-Beche, N., Parmentier, M., 1999. Physical and chemical properties of molecular compounds of lactose. J. Dairy Sci. 82, 2558–2563.

Du, B.Y., Tsui, O.K.C., Zhang, Q.L., He, T.B., 2001. Study of elastic modulus and yield strength of polymer thin films using atomic force microscopy. Langmuir 17, 3286–3291.

Durandurdu, M., Drabold, D.A., 2003. High-pressure phases of amorphous and crystalline silicon. Phys. Rev. B 67, 212101–212103.

Hancock, B.C., Clas, S.D., Christensen, K., 2000. Micro-scale measurement of the mechanical properties of compressed pharmaceutical powders. 1. The elasticity and fracture behaviour of microcrystalline cellulose. Int. J. Pharm. 209, 27–35.

Heuberger, M., Dietler, G., Schlapbach, L., 1995. Mapping the local Youngs modulus by analysis of the elastic deformations occurring in atomic-force microscopy. Nanotechnology 6, 12–23.

Jain, S., 1999. Mechanical properties of powders for compaction and tableting: an overview. Pharm. Sci. Technol. Today 2, 20–31.

Kwan, C.C., Chena, Y.Q., Ding, Y.L., Papadopoulos, D.G., Bentham, A.C., Ghadiri, M., 2004. Development of a novel approach towards predicting the milling behaviour of pharmaceutical powders. Eur. J. Pharm. Sci. 23, 327–336.

Levitas, V.I., 2004. A microscale model for strain-induced phase transformations and chemical reactions under high pressure. Europhys. Lett. 66, 687–693.

Liao, X.M., Wiedmann, T.S., 2004. Characterization of pharmaceutical solids by scanning probe microscopy. J. Pharm. Sci. 93, 2250–2258.

Liao, X.M., Wiedmann, T.S., 2005. Measurement of process-dependent material properties of pharmaceutical solids by nanoindentation. J. Pharm. Sci. 94, 79–92.

Narayan, P., Hancock, B.C., 2003. The relationship between the particle properties, mechanical behavior, and surface roughness of some pharmaceutical excipient compacts. Mater. Sci. Eng. A 355, 24–36.

Oliver, W.C., Pharr, G.M., 1992. An improved technique for determining hardness and elastic-modulus using load and displacement sensing indentation experiments. J. Mater. Res. 7, 1564–1583.

Podczeck, F., 2001. Investigations into the fracture mechanics of acetylsalicylic acid and lactose monohydrate. J. Mater. Sci. 36, 4687–4693.

Radmacher, M., Fritz, M., Cleveland, J.P., Walters, D.A., Hansma, P.K., 1994. Imaging adhesion forces and elasticity of lysozyme adsorbed on mica with the atomic-force microscope. Langmuir 10, 3809–3814.

Roberts, C.J., 2005. What can we learn from atomic force microscopy adhesion measurements with single drug particles? Eur. J. Pharm. Sci. 24, 153–157.

Sader, J., Larson, I., Mulvaney, P., White, 1995. Method for the calibration of atomic force microscope cantilevers. Rev. Sci. Inst. 66, 3789–3798.

Schmitt, E.A., Law, D., Zhang, G.G.Z., 1999. Nucleation and crystallization kinetics of hydrated amorphous lactose above the glass transition temperature. J. Pharm. Sci. 88, 291–296.

Sneddon, I.N., 1965. The relationship between load and penetration in the axisymmetric Boussineq problem for a punch of arbitrary profile. Int. J. Eng. Sci. 3, 47–57.

Taylor, L.J., Papadopoulos, D.G., Dunn, P.J., Bentham, A.C., Mitchell, J.C., Snowden, M.J., 2004. Mechanical characterisation of powders using nanoindentation. Powder Technol. 143/144, 179–185.

Ward, S., Perkins, M., Zhang, J.X., Roberts, C.J., Madden, C.E., Luk, S.Y., Patel, N., Ebbens, S.J., 2005. Identifying and mapping surface amorphous domains. Pharm. Res. 22, 1195–1202.

Williams, P.M., Shakesheff, K.M., Davies, M.C., Jackson, D.E., Roberts, C.J., Tendler, S.J.B., 1996. Blind reconstruction of scanning probe image data. J. Vac. Sci. Technol. B 14, 1557–1562.

Williams, P.M., Davies, M.C., Roberts, C.J., Tendler, S.J.B., 1998. Noise-compliant tip-shape derivation. Appl. Phys. A: Mater. Sci. Process. 66, S911–S914.

Wong, D.Y.T., Aulton, M.E., 1993. Elucidation of the mechanical characteristics of alpha-lactose single crystals from microindentation data.Elucidation of the mechanical characteristics of alpha-lactose single crystals from microindentation data. In: Wells, J.I., Rubinstein, M.H. (Eds.), Pharmaceutical Technology: Tableting Technology, vol. 2: Compression. Ellis Horwood, New York, pp. 169–186.

Zhang, J., Ebbens, S., Chen, X., Zheng, J., Luk, S., Madden, C., Patel, N., Roberts, C.J., 2006. Determination of the surface free energy of crystalline and amorphous lactose by atomic force microscopy adhesion measurement. Pharm. Res. 23, 401–407.